European Journal of Medicinal Chemistry 87 (2014) 267–273

Contents lists available at ScienceDirect

European Journal of Medicinal Chemistry

journal homepage: http://www.elsevier.com/locate/ejmech

Original article

Bioactivity of pyridine-2-thiolato-1-oxide metal complexes: Bi(III), Fe(III) and Ga(III) complexes as potent anti-*Mycobacterium tuberculosis* prospective agents

Ignacio Machado [a], Leonardo Biancolino Marino [b], Bruno Demoro [a], Gustavo A. Echeverría [c], Oscar E. Piro [c], Clarice Q.F. Leite [b], Fernando R. Pavan [b], Dinorah Gambino [a, *]

[a] Cátedra de Química Inorgánica, Departamento Estrella Campos, Facultad de Química, Universidad de la República, Gral. Flores 2124, 11800 Montevideo, Uruguay
[b] Faculdade de Ciencias Farmacêuticas, UNESP, 14801-902 Araraquara, SP, Brazil
[c] Departamento de Física, Facultad de Ciencias Exactas, Universidad Nacional de La Plata and IFLP (CONICET, CCT-La Plata), C.C. 67, 1900 La Plata, Argentina

ARTICLE INFO

Article history:
Received 9 June 2014
Received in revised form
15 September 2014
Accepted 21 September 2014
Available online 27 September 2014

Keywords:
Gallium(III)
Bismuth(III)
Iron(III)
Mycobacterium tuberculosis
Pyridine-2-thiol 1-oxide compounds

ABSTRACT

In the search for new therapeutic tools against tuberculosis and to further address the therapeutic potential of pyridine-2-thiol 1-oxide (Hmpo) metal complexes, two new octahedral $[M^{III}(mpo)_3]$ complexes, with M = Ga or Bi, were synthesized and characterized in the solid state and in solution. Attempts to crystallize $[Ga^{III}(mpo)_3]$ in CH_2Cl_2 led to single crystals of the reaction product $[GaCl(mpo)_2]$, where the gallium(III) ion is in a square basis pyramidal environment, *trans*-coordinated at the basis to two pyridine-2-thiolato 1-oxide anions acting as bidentate ligands through their oxygen and sulfur atoms.

The biological activity of the new $[M^{III}(mpo)_3]$ complexes together with that of the previously reported Fe(III) analogous compound and the pyridine-2-thiol 1-oxide sodium salt (Na mpo) was evaluated on *Mycobacterium tuberculosis*. The compounds showed excellent activity, both in the standard strain $H_{37}Rv$ ATCC 27294 (pan-susceptible) and in five clinical isolates that are resistant to the standard first-line anti-tuberculosis drugs isoniazid and rifampicin. These pyridine-2-thiol 1-oxide derivatives are promising compounds for the treatment of resistant tuberculosis.

© 2014 Elsevier Masson SAS. All rights reserved.

1. Introduction

Tuberculosis (TB) is an airborne and highly contagious infectious disease caused by *Mycobacterium tuberculosis* (MTB). Although TB is curable and preventable it still remains the second killing disease worldwide due to a single infectious agent after HIV/AIDS. In 2012 about 95% of the deaths occurred in low- and middle-income countries. About one-third of the world's population is infected but is not yet ill and cannot transmit the disease (latent TB). People bearing latent TB work as reservoir of the disease and those with compromised immune systems (HIV, malnutrition or diabetes) have a higher risk of getting ill [1,2]. Moreover, the increasing emergence of multi-drug resistant (MDR) and extensively drug resistant (XDR) MTB strains has also contributed to the alarming high morbidity and mortality of the disease [3,4]. Only few drugs are active against the *Mycobacterium* bacilli and MDR and XDR MTB organisms are virtually untreatable by the current drugs in immune compromised patients [5,6]. Although research on anti-TB drug development has substantially increased during the past decade, no new drug has already reached the pharmaceutical market [6]. Bedaquiline (Sirturo™) was approved in 2012 by the Food and Drug Administration but only for the treatment of resistant infections, mainly due to its side effects. New strategies need to evolve for the discovery of new drugs that could reduce the duration of the treatment, be active against resistant strains, do not interfere with antiretroviral drugs and be active against latent bacilli [7–9].

Inorganic Medicinal Chemistry could be a source of metal-based anti-TB drugs. In particular, we have successfully developed novel iron complexes with bioactive 3-aminoquinoxaline-2-carbonitrile

* Corresponding author.
E-mail address: dgambino@fq.edu.uy (D. Gambino).

http://dx.doi.org/10.1016/j.ejmech.2014.09.067
0223-5234/© 2014 Elsevier Masson SAS. All rights reserved.

N^1,N^4-dioxide derivatives as ligands that showed promising anti-MTB properties and improved activity as compared with the organic ligands [10–12]. At that stage iron (III) was selected as metal center taking into account the well known relationship between iron, mycobacteria and tuberculosis. In particular, it has been described that the treatment of mycobacteria with PAS (*p*-aminosalicylic acid), one of the oldest drugs against TB, resulted more effective when the cells were grown in media with adequate iron levels [13]. In addition, iron is needed by the bacteria and different iron complexes of bioactive ligands have shown anti-mycobacterial activity [10,12,14].

During the last years some of us have been studying the effect of metal coordination on the bioactivity of another aromatic amine *N*-oxide, namely pyridine-2-thiol 1-oxide (Fig. 1, Hmpo) [15–17]. Square planar complexes $[M^{II}(mpo)_2]$, where M(II) = Pd(II) or Pt(II), and a Au(I) homodinuclear mixed-ligand complex, $[Au^{I}_2(mpo)_2(PPh_3)_2]$, showed high activity on *Trypanosoma cruzi*, the protozoan parasite responsible of Chagas disease. Although they may have other intraparasite targets, the free ligand and the metal complexes inhibit the parasite specific enzyme NADH-fumarate reductase. This enzyme is responsible of the conversion of fumarate to succinate as energy source [15–18]. Generation of succinate through a similar enzymatic reductive process has been described in latent TB lung granulomas where the oxygen amount is severely limited. The utilization of the generated succinate enables MTB to maintain basic physiologic functions although it is not enough to allow growth [19].

Taking into account these antecedents and that we had previously assessed the high activity of mpo sodium salt on MTB, we decided to explore the effect of metal complexation on the anti-mycobacterial activity of structurally related octahedral mpo complexes by changing the metal center (Fe(III), Ga(III) or Bi(III)).

Fe(III) was the first choice metal center due to the arguments given above. Fe(III) and Ga(III) similarities have lead to potential biological competition between both metal ions *in vivo* [20–22]. Therefore, Ga(III) could be interesting for the development of drugs against MTB. On the other hand, Bi(III) shows an interesting bioinorganic chemistry, interacting with proteins in the iron binding sites, and its compounds have also shown medicinal applications, mainly as antimicrobial agents, but its anti-TB potentiality has not been explored yet [23–26].

In this work we further address the therapeutic potential of pyridine-2-thiolato 1-oxide metal complexes by synthesizing two new octahedral $[M^{III}(mpo)_3]$ complexes, with M = Ga or Bi. The complexes were characterized in the solid state and in solution by different techniques. Their biological activity together with that of the previously reported Fe(III) analogous compound and mpo sodium salt was evaluated on the *M. tuberculosis* standard strain H_{37}Rv ATCC 27294 (pan-susceptible) as well as on clinical isolates showing resistance to the standard drugs isoniazid and rifampicin.

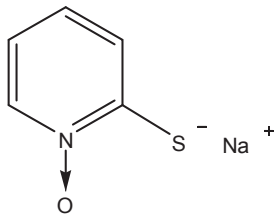

Fig. 1. Pyridine-2-thiol 1-oxide sodium salt (Na mpo).

2. Results and discussion

Two novel $[M^{III}(mpo)_3]$ complexes of the bioactive ligand pyridine-2-thiolato 1-oxide were synthesized with high purity and good yield by the reaction of the selected M(III) salt and pyridine-2-thiol 1-oxide sodium salt (Na mpo) in methanol at reflux. Unfortunately, it was impossible to obtain adequate single crystals of the complexes for structural crystallographic studies. Both were characterized by using elemental analyses, conductometric measurements, and FTIR and ^{1}H and ^{13}C NMR spectroscopy. $[Fe^{III}(mpo)_3]$ was synthesized with high purity and good yield by a different route to that previously reported and was characterized to assure its identity according to the literature [27].

Elemental analyses agree with the proposed formula. The molar conductivity value obtained for the complexes in DMSO solution shows that they are non-electrolytes, a fact that demonstrates the non-charged nature of the complexes [28]. No conductivity changes were observed during at least 7 days, hence suggesting that the complexes are stable in DMSO solution.

2.1. Characterization of the $[M^{III}(mpo)_3]$ complexes in the solid state and in solution

Characterization of the three complexes by FTIR and of Bi and Ga complexes by NMR spectroscopy has been performed and compared with the corresponding results for Na mpo and the previously reported Pd(II), Pt(II) and Au(I) complexes [15,16].

2.1.1. IR spectroscopic studies of the $[M^{III}(mpo)_3]$ complexes, **1**–**3**

Relevant IR absorption bands were tentatively assigned to molecular vibration modes (Table 1). The assignment of the typical bands due to ν(N–O), δ(N–O) and ν(C–S) modes is in agreement with those previously reported for Na mpo and other mpo metal complexes [15,16,29]. The frequency shift of these bands upon coordination to the metal is in agreement with the bidentate coordination of the ligand through the oxygen of the N–O group and the sulfur. Bands corresponding to metal-to-ligand stretching modes were also tentatively identified in the low wave number region (500–300 cm^{-1}) and assigned to ν (M–O) and ν (M–S) stretchs.

2.1.2. NMR characterization of the $[M^{III}(mpo)_3]$ complexes, **2**–**3**

Stability of the complexes in DMSO during at least 24 h was confirmed by NMR spectroscopy. Neither free ligand nor coordinated DMSO was detected. Table 2 shows the ^{1}H and ^{13}C NMR chemical shifts (δ) of Na mpo and the complexes and the chemical shift differences between them (expressed as $\Delta\delta$). The table also includes a figure showing the numbering scheme. ^{1}H NMR integrations and signal multiplicities were in agreement with the proposed formula and structure. HMQC and HMBC experiments allowed the assignment of all the signals of mpo and the investigated complexes. A deshielding effect of all the protons is observed due to electron withdrawing caused by coordination to the M(III) center. Upon coordination, the most distinguishing feature of the ^{13}C NMR spectra was the change in the chemical shift of carbon **1** which drops approximately from 168 to 156–159 ppm (Table 2). This result is in agreement with the previous report for Pd(II) and Pt(II) $[M^{II}(mpo)_2]$ complexes [16].

2.2. Crystal structure of $[GaCl(mpo)_2]$

Although $[GaCl(mpo)_2]$ complex is not of direct interest for the current work, the obtained $[GaCl(mpo)_2]$ single crystal affords a complete structural X-ray study to bring further support to the coordination mode of mpo to Ga(III) center and therefore its solid state molecular architecture is reported here. The partial

Table 1
Tentative assignment of the main characteristic IR bands of mpo sodium salt and the Fe, Ga and Bi [$M^{III}(mpo)_3$] complexes. Assignments for previously reported [$Pd^{II}(mpo)_2$] and [$Pt^{II}(mpo)_2$] complexes are included for comparison (wave numbers in cm^{-1}) [16].

Assignment	Na mpo	[$Fe^{III}(mpo)_3$]	[$Ga^{III}(mpo)_3$]	[$Bi^{III}(mpo)_3$]	[$Pd(mpo)_2$]	[$Pt(mpo)_2$]
ν(CH)	3068 m	3099 m	3103 m	3094 m	3095 m	3098 m
	3043 m	3067 m	3067 m	3072 m	3067 m	3085 m
		3023 m	3031 m	3023 m	3033 m	3059 m
ν(C=C)	1541 s	1539 vs	1545 vs	1540 vs	1547 vs	1551 vs
ν(N–O)	1206 s	1227 s	1226 s	1190 s	1247 s	1250 s
δ(N–O)	834 s	829 s	829 s	825 s	821 s	814 m
ν(C–S)	702 s	712 s	712 s	698 s	708 s/695 sh	711 s/686 sh
ν(M–O)	–	440 w	440 w	417 w	442 w	434 w
ν(M–S)	–	351 w	372 w	340 w	392 w	386 w
		342 w	353 w	318 w	313 w	300 w

ν: stretching; δ: bending; s: strong, m: medium; w: weak.

generation (few single crystals) of [$GaCl(mpo)_2$] from [$Ga(mpo)_3$] only when the crystallization is performed in CH_2Cl_2 could be probably explained considering that aliphatic halides like CH_2Cl_2 are likely to be contaminated with halogen acids from which they have been prepared [30].

Fig. 2 shows an ORTEP [31] drawing of the gallium complex. Intra-molecular bond distances and angles are given in Table 3. The Ga(III) ion is in a distorted square basis pyramidal coordination. It is *trans*-coordinated at the pyramid basis to two pyridine-2-thiolato 1-oxide anions acting as bidentate ligands through their O-atoms [Ga–O distances equal to 1.993(4) Å] and S-atoms [Ga–S distances of 2.2835(8) and 2.2763(9) Å]. The pyramid apex is occupied by a chloride ion [d(Ga–Cl) = 2.2248(9) Å]. As expected for an extended π-bonding delocalization, the ligands are planar [*rms* deviation of atoms from the best least-squares plane less than 0.016 Å]. The ligands slightly depart from mutual co-planarity [angled at 19.04(4)° from each other].

The observed inter-atomic distances and angles in the heterocycles are consistent with the description of their molecular structure in terms of resonant bonds. C–C bond distances are in the range from 1.351(4) to 1.396(4) Å and N–C lengths are in the 1.344(4)–1.374(4) Å interval. Single bonds N–O distances are 1.347(3) and 1.338(3) Å and C–S lengths are 1.717(3) and 1.710(3) Å.

2.3. Biological results

The analogous Ga(III), Fe(III) and Bi(III) compounds and the mpo sodium salt were evaluated on *M. tuberculosis*, both on the standard strain $H_{37}Rv$ ATCC 27294 (pan-susceptible) and on five clinical isolates with resistance already observed to the standard drugs isoniazid (INH) and rifampicin (RIF) (Table 4). All of them showed excellent activity either on $H_{37}Rv$ ATCC 27294 strain or on the INH and RIF resistant isolates (Tables 5 and 6).

In the field of drug discovery based on phenotypic screening, the first point to be observed is the activity of the compounds against the MTB H37Rv. The MIC (Minimal Inhibitory Concentration) results for the four *in vitro* evaluated compounds range from 1.06 μM to 3.29 μM (Table 5). The compounds show an equal or greater activity against the bacillus than drugs already used in therapy shown in the table. In a scheme of basic treatment recommended by the WHO (World Health Organization) the drugs used in a first phase are: isoniazid (MIC = 0.18 μM), rifampicin (MIC value around 0.49 μM), pyrazinamide (MIC value varying in the range of 48.74–406.14 μM at pH 5.5) and ethambutol (MIC = 2.45 μM) [32]. When we compare our results with the second line drugs or some new molecules in clinical trials, the expectation is even better (Table 5).

The Ga(III) complex was the most active among the compounds studied, being able to eliminate 90% of the bacteria in the *in vitro* assay at a concentration of 1.06 μM. This value is similar to those of molecules in Phase II of clinical development as SQ109, and is lower than those of molecules already in clinical use as streptomycin, ethambutol and moxifloxacin [32,33]. The Bi(III) complex showed the lower activity with a MIC value of 3.29 μM, but still qualifies as an excellent candidate for new anti-TB molecule as it presents a higher activity than pyrazinamide (at least 48.74 μM) and kanamycin (3.43 μM) [32]. Consequently, these compounds meet the first requirement of a new anti-TB molecule, showing significantly higher activity than the drugs already used in the treatment. They could be of great value (after further study) in an attempt to shorten the long drug therapy. Fe(III) and Ga(III) coordination of mpo led to an increase in activity.

Looking for satisfying the second anti-TB drug development criteria, the high activity of these compounds against the clinical isolates resistant to INH and RIF was also verified. The results were extremely promising (Table 6). A very striking fact is the similarity of the MIC values against resistant and sensitive strains for these compounds, which might indicate a different mechanism of action or target than those of INH and RIF. The Ga(III) and Fe(III) compounds were the most active complexes in the resistant strains, varying their strength according to the type of isolate. Their MIC values are extremely low in these strains that have been previously characterized by Miyata et al. [34] as highly resistant to the two main first-line anti-TB drugs. These results classify these compounds as candidates for drug discovery, meeting the second requirement needed for new anti-TB molecules. These results point at the tested pyridine-2-thiol 1-oxide compounds as promising new candidates against the major concern in the context of the disease: the emergence of resistance.

In order to get further insight into the potentiality of both most promising metal compounds, [$Ga(mpo)_3$] and [$Fe(mpo)_3$], their cytotoxicities on VERO epithelial cells (ATCC CCL81) was *in vitro* assayed. The IC_{50} values on these cells together with the selectivity indexes (SI = IC_{50} VERO cells (μM)/MIC *M. tuberculosis* $H_{37}Rv$ (μM)) where determined: IC_{50} Vero cells [$Ga(mpo)_3$] 10.04 μM, [$Fe(mpo)_3$] 4.61 μM; SI [$Ga(mpo)_3$] 9.37, [$Fe(mpo)_3$] 3.03. Usually a compound is considered promising for further testing if a SI close or higher than 10 is observed [35]. Accordingly, [$Ga(mpo)_3$] shows to be the most promising compound for further drug development. Mpo sodium salt showed a higher selectivity index than the metal complexes when considering Vero cells as mammalian cells model (SI = 80) but not if considering previous results on other mammalian cells like J774 macrophages (SI < 1) [16]. Nevertheless, the metal complexes showed much higher activities than Na mpo on pan-susceptible and resistant *M. tuberculosis* deserving therefore to perform further biological studies in order to establish their real therapeutic potentiality.

Table 2
^{1}H and ^{13}C NMR chemical shift values (δ) in ppm, of the ligand and the complexes, in DMSO-d_6:D_2O (9:1) at 30 °C.

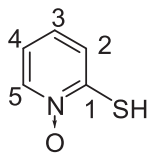

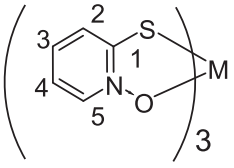

Proton	δ_H (multiplicity)					Carbon	δ_C				
	Ligand	$[Ga^{III}(mpo)_3]$	$\Delta\delta^a$	$[Bi^{III}(mpo)_3]$	$\Delta\delta^a$		Ligand	$[Ga^{III}(mpo)_3]$	$\Delta\delta^a$	$[Bi^{III}(mpo)_3]$	$\Delta\delta^a$
–	–	–	–		–	**1**	167.91	158.93	−8.98	155.90	−12.01
2	7.32 (d)	7.60 (d)	0.28	7.42 (d)	0.10	**2**	132.32	128.96	−3.36	131.26	−1.06
3	6.74 (t)	7.42 (t)	0.68	7.26 (t)	0.52	**3**	124.02	131.61	7.59	129.09	5.07
4	6.55 (t)	7.10 (t)	0.55	6.95 (t)	0.40	**4**	114.66	118.94	4.28	119.32	4.66
5	7.97 (d)	8.47 (d)	0.50	8.09 (d)	0.12	**5**	139.04	137.15	−1.89	140.15	1.11

[a] $\Delta\delta = (\delta_{Complex} - \delta_{Ligand})$. Multiplicity: d: doublet, t: triplet.

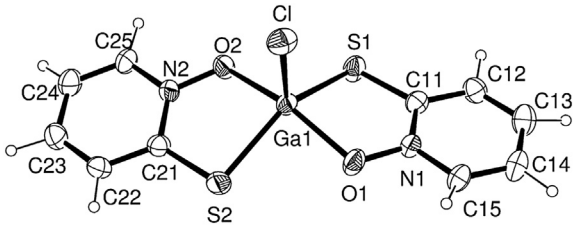

Fig. 2. Drawing of pyridine-2-thiolato 1-oxide gallium(III) complex, $[GaCl(mpo)_2]$, showing the labeling of the non-H atoms and their displacement ellipsoids at the 30% probability level.

Table 3
Bond lengths [Å] and angles [°] for $[GaCl(mpo)_2]$.

C(11)–N(1)	1.365(4)	N(1)–C(15)–C(14)	120.6(3)
C(11)–C(12)	1.387(4)	N(2)–C(21)–C(22)	116.4(3)
C(11)–S(1)	1.717(3)	N(2)–C(21)–S(2)	119.2(2)
C(12)–C(13)	1.363(5)	C(22)–C(21)–S(2)	124.4(3)
C(13)–C(14)	1.388(5)	C(23)–C(22)–C(21)	121.3(3)
C(14)–C(15)	1.352(5)	C(22)–C(23)–C(24)	119.9(4)
C(15)–N(1)	1.345(4)	C(25)–C(24)–C(23)	119.1(3)
C(21)–N(2)	1.374(4)	N(2)–C(25)–C(24)	120.9(4)
C(21)–C(22)	1.396(4)	N(1)–O(1)–Ga(1)	115.81(17)
C(21)–S(2)	1.710(3)	N(2)–O(2)–Ga(1)	116.31(17)
C(22)–C(23)	1.358(5)	O(2)–Ga(1)–O(1)	158.66(11)
C(23)–C(24)	1.381(5)	O(2)–Ga(1)–Cl	100.89(8)
C(24)–C(25)	1.351(4)	O(1)–Ga(1)–Cl	100.44(9)
C(25)–N(2)	1.344(4)	O(2)–Ga(1)–S(2)	85.57(6)
O(1)–N(1)	1.347(3)	O(1)–Ga(1)–S(2)	88.32(7)
O(1)–Ga(1)	1.993(2)	Cl––Ga(1)–S(2)	108.22(4)
O(2)–N(2)	1.338(3)	O(2)–Ga(1)–S(1)	86.82(7)
O(2)–Ga(1)	1.993(2)	O(1)–Ga(1)–S(1)	85.02(7)
Ga(1)–Cl	2.2248(9)	Cl–Ga(1)–S(1)	111.13(4)
Ga(1)–S(2)	2.2763(9)	S(2)–Ga(1)–S(1)	140.65(4)
Ga(1)–S(1)	2.2835(8)	C(11)–S(1)–Ga(1)	96.14(11)
		C(21)–S(2)–Ga(1)	96.30(11)
N(1)–C(11)–C(12)	116.5(3)	O(1)–N(1)–C(15)	116.4(3)
N(1)–C(11)–S(1)	118.8(2)	O(1)–N(1)–C(11)	120.6(2)
C(12)–C(11)–S(1)	124.7(3)	C(15)–N(1)–C(11)	122.9(3)
C(13)–C(12)–C(11)	121.4(4)	C(25)–N(2)–O(2)	117.2(3)
C(12)–C(13)–C(14)	119.7(4)	C(25)–N(2)–C(21)	122.3(3)
C(15)–C(14)–C(13)	118.9(3)	O(2)–N(2)–C(21)	120.5(2)

Although we cannot hypothesize about the mechanism of action of the metal complexes and the real role of metal coordination of this bioactive ligand, it is well known that coordination modifies electronic and physicochemical properties of bioactive organic ligands. These changes could lead to an improvement of the bioavailability of the organic drug. Moreover, metal complexes could act as drug transporters into the cell. In addition, coordination of a bioactive organic ligand could improve its activity through metal – drug synergism [36,37].

3. Conclusions

Two new $[M^{III}(mpo)_3]$ complexes, where M = Ga or Bi and mpo = pyridine-2-thiolato 1-oxide, were synthesized and characterized in the solid state and in solution. Both, together with pyridine-2-thiol 1-oxide sodium salt and the analogous $[Fe^{III}(mpo)_3]$ compound, were biologically evaluated on sensitive and resistant strains of *M. tuberculosis*.

In the field of drug discovery against tuberculosis, the pyridine-2-thiol 1-oxide derivatives tested in this work are promising compounds for the treatment of resistant tuberculosis and show high potentiality as hits in the development of new bioactive metal complexes series. Further studies are in progress to assess other relevant biological properties of these compounds.

4. Materials and methods

4.1. Materials

All common laboratory chemicals were purchased from commercial sources and used without further purification. Pyridine-2-thiol 1-oxide sodium salt (Na mpo), $FeCl_3$, $BiCl_3$ and $Ga(NO_3)_3$ $8.15H_2O$ were commercially available.

4.2. Syntheses of pyridine-2-thiolato-1-oxide-κS,κO metal complexes, $[M^{III}(mpo)_3]$, **1**–**3**

Complexes **1**–**3** were prepared by mixing a solution of Na mpo (43 mg, 0.29 mmol) in 8 mL MeOH with a solution of each metal(III) salt in 2 mL MeOH (0.094 mmol, 37 mg $Ga(NO_3)_3 \cdot 8.15H_2O$ or 15 mg $FeCl_3$ or 30.0 mg de $BiCl_3$). The reaction mixture was kept for 20 h under reflux. In each case a colored solid was isolated by centrifugation and washed with two portions of MeOH.

[Fe^{III}(mpo)$_3$],1. Yield: 31 mg, 77%. Black solid. Anal (%) calc. for $C_{15}H_{12}FeN_3O_3S_3$: C, 41.5; H, 2.8; N, 9.7; S, 22.1. Found: C, 41.4; H, 2.8, N, 9.7; S, 22.0. Λ_M(DMSO): 0.3 Scm^2 mol^{-1}.

[Ga^{III}(mpo)$_3$],2. Yield: 29 mg, 69%. Light yellow solid. Anal (%) calc. for $C_{15}H_{12}GaN_3O_3S_3$: C, 40.2; H, 2.7; N, 9.4; S, 21.4. Found: C, 40.0; H, 2.7, N, 9.3; S, 21.2. Λ_M(DMSO): 2.0 Scm^2 mol^{-1}.

Table 4
Phenotypic and genotypic resistance profiles related to isoniazid (INH) and rifampicin (RIF) of the clinical isolates used in the REMA assays [34].

Clinical isolate	BACTEC		REMA		Sequencing			
			MIC (μg/mL)		Genes related to INH resistance			Gene related to RIF resistance
	INH	RIF	INH	RIF	*inhA*	*katG*	*ahpC*	*rpoβ*
1	R	R	>25.00	>25.00	*	Ser315Thr	*	Pro445Leu/Pro526Leu
2	R	R	>25.00	>25.00	*	*	*	C → G in the positions 450 and 531
3	R	R	>25.00	>25.00	*	Ser315Thr	*	C → T in the positions 450 and 531
4	R	S	>25.00	0.212	*	*	*	*
5	R	R	>25.00	>25.00	C → T in the position −15	*	*	C → T in the positions 450 and 531

R: resistant; S: sensitive; C: citosine; T: timine; G: guanine.
Mutations of N → N type (where *N* is an arbitrary nitrogenous base) indicate a silent mutation in which there was not an amino acid exchange.

[Bi^{III}(mpo)$_3$],3. Yield: 49 mg, 90%. Yellow solid. Anal (%) calc. for $C_{15}H_{12}BiN_3O_3S_3$: C, 30.7; H, 2.1; N, 7.2; S, 16.4. Found: C, 30.6; H, 2.0, N, 7.1; S, 16.2. Λ_M(DMSO): 0.5 Scm^2 mol^{-1}.

4.3Physicochemical characterization

C, H, N and S analyses were carried out with a Thermo Scientific Flash 2000 elemental analyzer. Conductometric measurements were done over time (7 days) at 25 °C in 10^{-3} M DMSO solutions using a Conductivity Meter 4310 Jenway to determine the type of electrolyte and to assess the stability of the complexes in such medium [28]. The FTIR absorption spectra (4000–300 cm^{-1}) of the complexes and the free ligand were measured as KBr or CsI pellets with a Shimadzu IRPrestige-21 instrument. ^{1}H NMR and ^{13}C NMR spectra of Na mpo and the complexes were recorded in DMSO-d_6:D_2O (9:1) at 30 °C on a Bruker DPX-400 instrument (at 400 MHz and 100 MHz, respectively). Hetero-nuclear correlation experiments (2D-HETCOR), HSQC (hetero-nuclear single quantum correlation) and HMBC (hetero-nuclear multiple bond correlation), were carried out with the same instrument. Tetramethylsilane was used as the internal standard. Chemical shifts are reported in ppm.

4.4. Crystallographic study of [GaCl(mpo)$_2$]

When attempting to obtain [Ga(mpo)$_3$] adequate crystals for structural X-ray diffraction studies, re-crystallization in CH_2Cl_2 rather led to single crystals of the reaction product [GaCl(mpo)$_2$]. The X-ray measurements were performed on an Oxford Xcalibur Gemini, Eos CCD diffractometer with graphite-monochromated CuKα (λ = 1.54184 Å) radiation. X-ray diffraction intensities were collected (ω scans with ϑ and κ-offsets), integrated and scaled with CrysAlisPro suite of programs [38]. The unit cell parameters were obtained by least-squares refinement (based on the angular settings for all collected reflections with intensities larger than seven times the standard deviation of measurement errors) using CrysAlisPro. Data were corrected empirically for absorption employing the multi-scan method implemented in CrysAlisPro. The structure was solved by direct methods with SHELXS-97 [39] and the corresponding molecular model developed by alternated cycles of Fourier methods and full-matrix least-squares refinement on F^2 with SHELXL-97 [40]. The hydrogen atoms were positioned on stereo-chemical basis and refined with the riding model. Crystal data, data collection procedure, structure determination methods and refinement results are summarized in Table 7. Crystallographic structural data have been deposited at the Cambridge Crystallographic Data Centre (CCDC). Any request to the CCDC for this material should quote the full literature citation and the reference number CCDC 817624.

4.5. Biological activity

4.5.1. Determination of Minimal Inhibitory Concentration (MIC)

The anti-MTB activity of the compounds was determined by the REMA (Resazurin Microtiter Assay) method [41]. Stock solutions of the tested compounds were prepared in DMSO and diluted in Middlebrook 7H9 broth (Difco) supplemented with oleic acid, albumin, dextrose and catalase (OADC enrichment – BBL/Becton–Dickinson), to obtain final drug concentration ranges of 0.09–25 μg/mL. Isoniazid was dissolved in distilled water and rifampicin in DMSO, and both were used as standard drugs. A suspension of the MTB H_{37}Rv ATCC 27294 and five clinical isolates resistant to isoniazid and rifampicin were cultured in Middlebrook 7H9 broth supplemented with OADC and 0.05% Tween 80. The cultures were frozen at −80 °C in aliquots. After two days the CFU/mL (colony formation unit/mL) of an aliquot was determined. The concentrations were adjusted by 5 × 10^5 CFU/mL and 100 μL of the inoculum were added to each well of a 96-well micro-plate together with 100 μL of the compounds. Samples were set up in triplicate. The plates were incubated for 7 days at 37 °C. After 24 h, 30 μL of 0.01% resazurin (solubilized in water) was added. The fluorescence of the wells was read after 24 h with a TECAN Spectrafluor®. The MIC was defined as the lowest concentration resulting in 90% inhibition of growth of MTB.

Table 5
MIC values of the mpo compounds against *M. tuberculosis* H_{37}Rv compared to MIC values of first- and second-line anti-TB drugs, other drugs also used in the treatment and new proposed molecules [32].

Compound	MIC value against *M. tuberculosis* H_{37}Rv	
	μg mL^{-1}	μM
Na mpo	0.36 ± 0.01	2.42
[Ga(mpo)$_3$]	0.48 ± 0.00	1.06
[Bi(mpo)$_3$]	1.47 ± 0.03	3.29
[Fe(mpo)$_3$]	0.66 ± 0.08	1.53
Isoniazid	0.02	0.18
Rifampicin	0.40	0.49
Pyrazinamide	6.00–50.00[a]	48.74–406.14[a]
Ethambutol	0.50	2.45
Streptomycin	1.00	1.72
Amikacin	0.50–1.00	0.85–1.70
Capreomycin	2.00	2.61
Kanamycin	2.00	3.43
Gatifloxacin	0.25	0.67
Moxifloxacin	0.50	1.14
Bedaquiline	0.06	0.11
Linezolid	0.25	0.74
SQ109	0.35	1.06
PA-824	0.15–0.30	0.42–0.84
Clofazimine	0.10	0.21
Para-aminosalicylic acid	0.30–1.00	1.96–6.53

[a] At pH 5.5.

Table 6
MIC values of the compounds against the resistant clinical isolates listed above in Table 4. The first value represents the MIC in μg mL^{-1}, while the second represents the MIC value in μM.

Compound	MIC values against resistant clinical isolates 1–5 (μg mL^{-1}/μM)				
	1	**2**	**3**	**4**	**5**
Na mpo	0.71/4.76 ± 0.03	0.35/2.38 ± 0.00	0.73/4.90 ± 0.03	0.59/3.95 ± 0.07	0.38/2.58 ± 0.01
[Ga(mpo)$_3$]	0.74/1.66 ± 0.00	0.42/0.94 ± 0.85	0.76/1.70 ± 0.76	0.91/2.03 ± 0.30	0.46/1.02 ± 0.10
[Bi(mpo)$_3$]	1.98/3.37 ± 0.84	1.46/2.49 ± 0.84	12.43/21.18 ± 0.30	2.90/4.94 ± 0.25	3.22/5.49 ± 2.05
[Fe(mpo)$_3$]	0.62/1.42 ± 0.21	0.35/0.80 ± 0.00	1.07/2.46 ± 0.22	0.97/2.23 ± 0.38	0.43/0.99 ± 0.12

4.5.2. Cytotoxicity assay

In vitro cytotoxicity assays were performed on VERO epithelial cells (ATCC CCL81). This lineage is widely used for phenotypic screening of drugs being regarded as a normal cell derived from normal human epithelial tissue [42]. The cells were routinely maintained in DMEM complete medium supplemented with 10% heat inactivated fetal bovine serum (FBS) plus gentamicin (50 mg/L) and amphotericin B (2 mg/L) at 37 °C, in a humidified 5% CO_2 atmosphere. After reaching confluence, the cells were detached and counted. For the cytotoxicity assay, 1×10^5 cells/mL were seeded in 200 μL of complete medium in 96-well plates (NUNC™). The plates were incubated under the same conditions for 24 h to allow cell adhesion prior to drug testing. The compounds were dissolved in DMSO (5%) and subjected to two-fold serial dilution from 500 to 3.9 μg/mL. The cells were exposed to the compounds at various concentrations for 24 h. Resazurin solution was then added to the cell cultures and incubated for 6 h. Cell respiration, as an indicator of cell viability, was detected by reduction of resazurin to resorufin, whose pink color and fluorescence indicate cell viability. A persistent blue color of resazurin is a sign of cell death. The fluorescence measurements (530 nm excitation filter and 590 nm emission filter) were performed in a SPECTRAfluor Plus (Tecan) microfluorimeter. The IC_{50} value was defined as the highest drug concentration at which 50% of the cells are viable relative to the control. Each test was set up in triplicate. The selectivity index (SI) was calculated by dividing IC_{50} for the VERO cells by the MIC for the pathogen.

Table 7
Crystal data and structure refinement results for chloride bis(pyridine-2-thiolato-1-oxide-κ*S*,κ*O*) gallium(III) complex, [GaCl(mpo)$_2$].

Empirical formula	C_{10} H_8 Cl Ga N_2 O_2 S_2
Formula weight	357.47
Temperature	293(2) K
Wavelength	1.54184 Å
Crystal system	Orthorhombic
Space group	*Pbca*
Unit cell dimensions	$a = 13.9373(9)$ Å $b = 12.7865(7)$ Å $c = 14.4427(7)$ Å
Volume	2573.8(3) Å^3
Z, density (calculated)	8, 1.845 Mg/m^3
Absorption coefficient	7.841 mm^{-1}
F(000)	1424
Crystal size	0.236 × 0.095 × 0.038 mm^3
Theta range for data collection	5.61–73.95°
Index ranges	$-8 \le h \le 17$, $-13 \le k \le 15$, $-16 < l \le 18$
Reflections collected	8233
Independent reflections	2600 [R(int) = 0.0318]
Observed reflections	1482
Completeness to $q = 73.95°$	99.8%
Refinement method	Full-matrix least-squares on F^2
Data/restraints/parameters	2600/0/171
Goodness-of-fit on F^2	0.862
Final R indices[a] [$I > 2\sigma(I)$]	$R1 = 0.0314$, $wR_2 = 0.0805$
R indices (all data)	$R1 = 0.0591$, $wR_2 = 0.0900$
Largest diff. peak and hole	0.711 and −0.259 e.Å^{-3}

[a] $R_1 = \Sigma||F_o|-|F_c||/\Sigma|F_o|$, $wR_2 = [\Sigma w(|F_o|^2-|F_c|^2)^2/\Sigma w(|F_o|^2)^2]^{1/2}$.

Acknowledgments

Authors would like to thank RIIDFCM (209RT0380) CYTED network for supporting collaborative research on development of bioactive metal-based compounds, Conselho Nacional de Desenvolvimento Científico e Tecnológico (CNPq/Glaxo ref. Process: 406827/2012-5), Coordenação de Aperfeiçoamento de Pessoal de Nível Superior (CAPES), Pró-Reitoria de Pesquisa/UNESP (PROPE ref. Process: 0102/004/43) and Fundação de Amparo à Pesquisa do Estado de São Paulo (FAPESP ref. Process: 2011/21232-1). I.M. acknowledges the support of the Agencia Nacional de Investigación e Innovación (ANII, Uruguay) grant INI_X_2011_1_3902. The crystallographic work was supported by CONICET (PIP 1529) and ANPCyT (PME06 2804 and PICT06 2315) of Argentina. G.A.E. and O.E.P are Research Fellows of CONICET.

Appendix A. Supplementary data

Supplementary data related to this article can be found at http://dx.doi.org/10.1016/j.ejmech.2014.09.067.

References

[1] http://www.who.int/topics/tuberculosis/en/visited 27/12/2013.
[2] WHO Global Tuberculosis Report, 2013.
[3] P.G. Smith, A.R. Moss, Epidemiology of tuberculosis, in: B.R. Bloom (Ed.), Tuberculosis, Pathogenesis, Protection and Control, ASM Press, Washington, 1994, pp. 47–61.
[4] A. Zwerling, M.A. Behr, A. Verma, T.F. Brewer, D. Menzies, M. Pai, Plos Med. 8 (2011), http://dx.doi.org/10.1371/journal.pmed.1001012.
[5] N.R. Gandhi, P. Nunn, K. Dheda, H.S. Schaaf, M. Zignol, D. van Soolingen, P. Jensen, J. Bayona, Lancet 375 (2010) 1830–1843.
[6] Z. Ma, C. Lienhardt, H. McIlleron, A. J Nunn, X. Wang, Lancet 357 (2010) 2100–2109.
[7] A. Koul, E. Arnoult, N. Lounis, J. Guillemont, K. Andries, Nature 469 (2011) 483–490.
[8] C. Lienhardt, A. Vernon, M.C. Raviglione, Curr. Op. Pulm. Med. 16 (2010) 186–193.
[9] M. Coffee, Future Med. (2013), http://dx.doi.org/10.2217/ebo.12.500.
[10] M.B. Tarallo, C. Urquiola, A. Monge, B. Parajón Costa, R.R. Ribeiro, A.J. Costa-Filho, R.C. Mercader, F.R. Pavan, C.Q.F. Leite, M.H. Torre, D. Gambino, J. Inorg. Biochem. 104 (2010) 1164–1170.
[11] Patent request PI0902923-0 Protocolo 018090038618, Brazil. Complexos de ferro (Fe(II) e Fe(III)) com quinoxalina N^1,N^4-dioxido derivados: Síntese, caracterizaçao e atividade antimicrobiana.
[12] M.B. Tarallo, C. Urquiola, A. Monge, F.R. Pavan, C.Q. Leite, M.H. Torre, D. Gambino, Metal. Ions Biol. Med. 10 (2008) 865–872.
[13] C. Ratledge, Tuberculosis 84 (2004) 110–130.
[14] J.S. Oliveira, E.H.S. Souza, L.A. Basso, M. Palaci, R. Dietze, D.S. Santos, I.S. Moreira, Chem. Comm. (2004) 312–313.
[15] M. Vieites, P. Smircich, L. Guggeri, E. Marchán, A. Gómez-Barrio, M. Navarro, B. Garat, D. Gambino, J. Inorg. Biochem. 103 (2009) 1300–1306.
[16] M. Vieites, P. Smircich, B. Parajón-Costa, J. Rodríguez, V. Galaz, C. Olea-Azar, L. Otero, G. Aguirre, H. Cerecetto, M. González, A. Gómez-Barrio, B. Garat, D. Gambino, J. Biol. Inorg. Chem. 13 (2008) 723–735.
[17] A. Merlino, M. Vieites, D. Gambino, E.L. Coitiño, J. Mol. Graph. Mod. 48 (2014) 47–59.
[18] J.F. Turrens, C.L. Newton, L. Zhong, F.R. Hernández, J. Whitfield, R. Docampo, FEMS Microbiol. Lett. 175 (1999) 217–221.

[19] S. Watanabe, M. Zimmermann, M.B. Goodwin1, U. Sauer, C.E. Barry, H.I. Boshoff, PLoS Pathog. 7 (2011) e1002287.
[20] E.J. Baran, Lat. Am. J. Pharm. 27 (2008) 776–779.
[21] P. Collery, B. Keppler, C. Madoulet, B. Desoize, Crit. Rev. Oncol. Hematol. 42 (2002) 283–296.
[22] F. Silva, F. Marques, I.C. Santos, A. Paulo, A.S. Rodrigues, J. Rueff, I. Santos, J. Inorg. Biochem. 104 (2010) 523–532.
[23] R. Ge, H. Sun, Acc. Chem. Res. 40 (2007) 267–274.
[24] G.G. Briand, N. Burford, Chem. Rev. 99 (1999) 2601–2657.
[25] E.R.T. Tiekink, Crit. Rev. Oncol. Hematol. 42 (2002) 217–224.
[26] Y. Yamamoto, K. Ohdoi, X. Chen, M. Kitano, K. Akiba, Organometallics 12 (1993) 3297–3303.
[27] X. Chen, Y. Hu, D. Wu, L. Weng, B. Kang, Polyhedron 10 (1991) 2651–2657.
[28] W.J. Geary, Coord. Chem. Rev. 7 (1971) 81–122.
[29] B.S. Parajón-Costa, A.C. González-Baró, E.J. Baran, Z. Anorg. Allg. Chem. 628 (2002) 1419–1424.
[30] W.L.F. Armarego, D.D. Perrin, Purification of Laboratory Chemicals, fourth ed., Butterworth-Heinemann, Oxford, England, 1996, p. 68.
[31] C.K. Johnson, ORTEP-II. A Fortran Thermal-Ellipsoid Plot Program, Report ORNL-5318, Oak Ridge National Laboratory, Tennessee, USA, 1976.
[32] Handbook of anti-tuberculosis agents, Tuberculosis 88 (2008) 85–169.
[33] H. Boshoff, K. Tahlan, Drugs Future 38 (2013) 467–474.
[34] M. Miyata, F.R. Pavan, D.N. Sato, L.B. Marino, M.H. Hirata, R. Fressati Cardoso, F.A. Fiúza de Melo, C.F. Zanelli, C. Queico, F. Leite, Biomed. Pharmacother. 65 (2011) 456–459.
[35] I. Orme, Antimicrob. Agents Chemother. 45 (2001) 1943–1946.
[36] R.A. Sánchez-Delgado, A. Anzellotti, L. Suárez, Metal complexes as chemotherapeutic agents against tropical diseases: malaria, trypanosomiasis, and leishmaniasis, in: Metal Ions in Biological Systems, vol. 41, Marcel Dekker, New York, 2004, pp. 379–419.
[37] M. Navarro, C. Gabbiani, L. Messori, D. Gambino, Drug Discov. Today 15 (2010) 1070–1078.
[38] CrysAlisPro, Oxford Diffraction Ltd., Version 1.171.33.48 (Release 15-09-2009 CrysAlis171.NET).
[39] G.M. Sheldrick, SHELXS-97. Program for Crystal Structure Resolution, Univ. of Göttingen, Göttingen, Germany, 1997;
See also: G.M. Sheldrick Acta Crystallogr. A 46 (1990) 467–473.
[40] G.M. Sheldrick, SHELXL-97. Program for Crystal Structures Analysis, Univ. of Göttingen, Göttingen, Germany, 1997;
See also: G.M. Sheldrick Acta Crystallogr. A 64 (2008) 112–122.
[41] J.C. Palomino, A. Martin, M. Camacho, H. Guerra, J. Swings, F. Portaels, Antimicrob. Agents Chemother. 46 (2002) 2720–2722.
[42] F.R. Pavan, P.I. da S. Maia, S.R. Leite, V.M. Deflon, A.A. Batista, D.N. Sato, S.G. Franzblau, C.Q. Leite, Eur. J. Med. Chem. 45 (2010) 1898–1905.